The Astrophysical Journal, 594:L67–L70, 2003 September 10

THE SPECTRUM OF THE COSMIC MICROWAVE BACKGROUND ANISOTROPY FROM THE COMBINED *COBE*[1] FIRAS AND *WMAP* OBSERVATIONS

D. J. Fixsen[2]

Received 2003 May 22; accepted 2003 July 25; published 2003 August 8

ABSTRACT

The cosmic microwave background (CMB) anisotropy data from the *COBE* Far Infrared Absolute Spectrophotometer (FIRAS) is reanalyzed in light of the *Wilkinson Microwave Anisotropy Probe* (*WMAP*) observations. The frequency spectrum of the FIRAS signal that has the spatial distribution seen by *WMAP* is shown to be consistent with CMB temperature fluctuations well into the Wien region of the spectrum. The consistency of these data, from very different instruments with very different observing strategies, provides compelling support for the interpretation that the signal seen by *WMAP* is temperature anisotropy of cosmological origin. The data also limit rms fluctuations in the Compton y parameter, observable via the Sunyaev-Zeldovich effect, to $\Delta y < 3 \times 10^{-6}$ (95% confidence level) on $\sim 5°$ angular scales.

Subject headings: cosmic microwave background — cosmology: observations

1. INTRODUCTION

The spectrum of the anisotropy observed by the *COBE* Differential Microwave Radiometers (DMR) was examined by Fixsen et al. (1997) using the *COBE* Far Infrared Absolute Spectrophotometer (FIRAS) data and found to be roughly consistent with thermal emission. The recent results of the *Wilkinson Microwave Anisotropy Probe* (*WMAP*; Bennett et al. 2003b) offer several advantages in this examination. First, *WMAP* has a small beam, so the comparison can be made on the angular resolution of the FIRAS instrument. Second, the *WMAP* data have lower noise, so comparison will have lower noise. Third, the *WMAP* results have an improved Galaxy model (Bennett et al. 2003c), which allows both larger sky coverage and reduced systematic errors. Each of these improves the comparison, so the new result has less than half of the uncertainty of the former result.

The *WMAP* (Bennett et al. 2003a and references therein) was designed to measure anisotropy in the cosmic microwave background (CMB) temperature on $\sim 0.^{\circ}2$ and larger angular scales. The precise measurement of anisotropy provides important information on conditions in the early universe. The signal seen by *WMAP* is widely interpreted to be of primordial cosmological origin. As such, it provides key information on gravitational potential fluctuations in the early universe that presumably served as the seeds for the formation of large-scale structure. The primary evidence that the anisotropy is cosmological arises from a spectral analysis of the five *WMAP* frequency channels at 22.77, 33.02, 40.72, 60.75, and 93.53 GHz. Cosmological anisotropy is predicted to have a Planckian spectrum of the form $I(\nu) = B(\nu, T_0) + \Delta T \partial B(\nu, T)/\partial T$, where $T_0 = 2.725$ K is the mean temperature of the CMB (Mather et al. 1999), $B(\nu, T)$ is the Planck function at temperature T, and $\Delta T = T - T_0$ is the temperature anisotropy in a given direction in the sky. The *WMAP* anisotropy data are consistent with a Planck spectrum and are inconsistent with any known Galactic emission (Hinshaw et al. 2003). However, the frequency range covered by *WMAP* is relatively limited, and observations of the anisotropy into the Wien region of the spectrum strengthen the view that the anisotropy is due to temperature fluctuations in the CMB.

The FIRAS instrument aboard the *COBE* satellite (Mather et al. 1994) was designed to measure the spectrum of the CMB. The FIRAS observations demonstrate that the spectrum of the uniform (monopole) component of the CMB is Planckian to 50 parts per million (ppm) of the peak radiation intensity (Fixsen et al. 1996). Moreover, the CMB dipole exhibits a Planck spectrum ($\partial B/\partial T$) to high precision (Fixsen & Mather 2002 and references therein). In this Letter we reassess the spectrum and spatial distribution of the higher order anisotropy in the FIRAS data.

The measurement of the anisotropy spectrum is difficult because the intrinsic anisotropy is weak, roughly one part in 10^5 of the intrinsic CMB brightness, and near the limits of the FIRAS sensitivity and stability; i.e., it is difficult to make absolute measurements of the CMB that are stable to 0.001% over the course of a year of observations. In addition, in the Wien region of the spectrum the signal becomes dominated by emission from interstellar dust. To overcome these difficulties our analysis employs data from the Diffuse Infrared Background Experiment (DIRBE) instrument to characterize the dust that would otherwise confuse the measurement. The *WMAP* data provide the spatial distribution of the anisotropy, which effectively modulates the FIRAS spectral data, significantly reducing the systematic effects.

The *WMAP* and DIRBE maps convolved with the FIRAS beam are used as spatial templates to which the FIRAS data are fitted. The result is a mean spectrum per map of the emission traced by that map. The mean spectrum corresponding to the *WMAP* anisotropy is compared with the Planck spectrum given above.

2. THE DATA

The FIRAS data consist of spectra between 2 and 21 $\mathrm{cm^{-1}}$ (0.5 cm to 480 μm wavelength) in each of 6063 pixels on the sky (there are 6144 pixels in the full Quadcube sky; O'Neill & Laubscher 1976). They were calibrated using the method described by Fixsen et al. (1994), with the improvements noted by Fixsen et al. (1996). A weighted average of all of the low-frequency FIRAS data was used. The FIRAS data have 7° angular resolution, as measured by its FWHM, but it is not

[1] The National Aeronautics and Space Administration Goddard Space Flight Center (NASA/GSFC) was responsible for the design, development, and operation of the *Cosmic Background Explorer* (*COBE*).

[2] SSAI, Code 685, NASA Goddard Space Flight Center, Greenbelt, MD 20771; fixsen@stars.gsfc.nasa.gov.

Gaussian; the FIRAS beam more closely resembles a top-hat profile. This admits higher spatial frequencies, which makes the spatial response of the FIRAS beam closer to a 5° Gaussian beam. This analysis takes advantage of the full resolution of the FIRAS beam.

A modification of the "internal linear combination" *WMAP* temperature map described by Bennett et al. (2003b) is used. The "internal linear combination" is a weighted average of all 20 *WMAP* channel maps designed to remove the foreground the Galactic synchrotron, free-free, and dust emission contamination. This *WMAP* map was convolved with the FIRAS beam and converted to Quadcube format in ecliptic coordinates. The *WMAP* beams are much smaller (*K* band 49′ to *V* band 13′), so neither the repixelization or the details of the *WMAP* beams are important on the scale of the FIRAS beam. After convolution, the rms of the *WMAP* is 39 μK.

The DIRBE data (*COBE* DIRBE Explanatory Supplement 1997)[3] were also convolved with the FIRAS beam prior to fitting. The long-wavelength DIRBE data were corrected for low-level emission from interplanetary (zodiacal) dust by interpolating to the response at a solar elongation of 90° corresponding to the FIRAS pointing. This analysis uses the 100 and 240 μm DIRBE maps rather than the higher noise 140 μm DIRBE map, although the final results are very similar using any pair.

3. SPECTRAL ANALYSIS

The FIRAS sky spectra are a function of frequency and position: $S(l, b; \nu)$, where l and b are Galactic coordinates and ν is frequency. Since the data are binned into discrete pixels, p, and frequencies, ν, we write the FIRAS data as $S_{p\nu}$. To investigate the CMB anisotropy, we model the dominant emission components in the data by assuming the frequency and spatial dependences are separable, as follows:

$$M_{p\nu} = u_\nu + D_p d_\nu + G_p g_\nu + H_p h_\nu + A_p a_\nu, \qquad (1)$$

where M denotes our model of the data S. The CMB monopole is represented by the uniform spectrum u_ν; the CMB dipole anisotropy is represented by the spatial distribution D_p and the spectrum d_ν. Galactic emission is modeled using two spatial templates, G_p and H_p, and two spectra g_ν and h_ν. The spatial template, A_p, is the CMB′ anisotropy map from Bennett et al. with an associated spectrum a_ν. In this analysis, the spatial templates above are fixed and a least-squares fit of the data is performed to determine the spectra, u, d, g, h, and a, at each frequency.

The spatial templates D_p, G_p, and H_p are specified as follows. The dipole is given by $D_p = \cos\theta$, where θ is the angle between the direction of observation and the dipole direction, $(l, b) = (264.^\circ26, +48.^\circ22)$ (Bennett et al. 1996). The small differences ($\sim0.^\circ3$) between the *WMAP*, FIRAS, and DMR dipole directions are within their uncertainties and are negligible this analysis. For the two Galactic templates we use the 240 and 100 μm DIRBE maps convolved to the FIRAS beam profile. The use of two templates simultaneously allows for modest spatial variations in the Galactic dust spectrum and for a possible far-infrared background. To give the derived spectra common units of MJy sr^{-1}, we normalize the spatial templates to be dimensionless. The dipole map is scaled to range from -1 to $+1$. The Galaxy maps are scaled such that the average value over the polar caps ($|b| > 60°$) is 1.07, corresponding to the mean of csc $|b|$ over the same region. The resulting Galaxy spectrum roughly gives the intensity at the Galactic poles.

We normalize the *WMAP* map to roughly unit rms by dividing it by 39 μK, the estimated rms of the anisotropy after convolving with the FIRAS beam. This allows us to compare the derived anisotropy spectrum with the previously derived spectra using consistent units. We denote the normalized map A_p. The residual systematic errors and the small noise in the *WMAP* data are ignored in this analysis. Systematic errors are only evident in this map at the Galactic center, which is excluded anyway.

For the fit we define χ^2 to be

$$\chi^2_\nu = \sum_{pp'} [S_{p\nu} - M_{p\nu}(u, d, g, h, a)] \times W_{pp'}[S_{p'\nu} - M_{p'\nu}(u, d, g, h, a)]/\sigma^2_\nu, \qquad (2)$$

where p and p' are sky pixel indices, W is the inverse of the pixel-pixel covariance of the FIRAS data, including correlations introduced by the calibration and "destriping" processes, and σ_ν is the factorable uncertainty of the spectrum at frequency ν, including "glitch" effects (see Fixsen et al. 1996). This χ^2 is minimized independently at each frequency to determine the mean spectra u, d, g, h, and a. It is important to note that this fit makes no a priori assumptions about the forms of these spectra; only their spatial distributions are posited. Note also that σ^2_ν does not affect the best-fit intensity at each frequency, only the uncertainty estimate. The FIRAS data have been processed in such a way as to maintain the separability of the positional and the spectral uncertainties.

For the discussion following, data with $|b| < 10°$ have been excluded, although other Galactic cuts were examined. Observations in which the FIRAS beam catches Galactic plane are complicated both by the details of the pointing and by the Galactic plane. There are 5010 pixels ($\sim2.^\circ6$ square) remaining in the data after applying the 10° Galaxy cut and excising the pixels not observed by FIRAS. The derived spectra and uncertainties are shown in Figure 1. The correlation matrix of the elements is given in Table 1. The table shows only modest correlations between the anisotropic component and any of the others, as is expected for a random background fluctuation.

The monopole and dipole spectra have been discussed extensively by Fixsen et al. (1996); this work does not alter any of their conclusions. The Galactic spectra (Fig. 1*c*) are the shape one would expect for dust at ∼15 K. The negative spectrum for the 100 μm map is a natural consequence of a frequency extrapolation that does not account for a varying dust temperature. Indeed, if the dust temperature were constant, the (normalized) 240 and 100 μm maps would be identical and the fit would be degenerate. To study the Galactic dust emission one should look at the higher frequencies and lower latitudes; here we are interested only in removing the dust emission.

There is a significant detection of signal correlated with the *WMAP* anisotropy (Fig. 1*d*): the χ^2 for zero signal is 305 for 43 dof, while a $(\partial B_\nu/\partial T)$ spectrum normalized to the *WMAP* results gives a χ^2 of 49. This strongly suggests that the anisotropy observed by WMAP, and corroborated by FIRAS, is due to temperature variations in the CMB.

The effects of the FIRAS gain variations and other nonlinear effects are entirely negligible because of the small amplitude of the anisotropy. Most instrumental systematic effects are sup-

[3] See http://nssdcftp.gsfc.nasa.gov/spacecraft_data/cobe/dirbe.

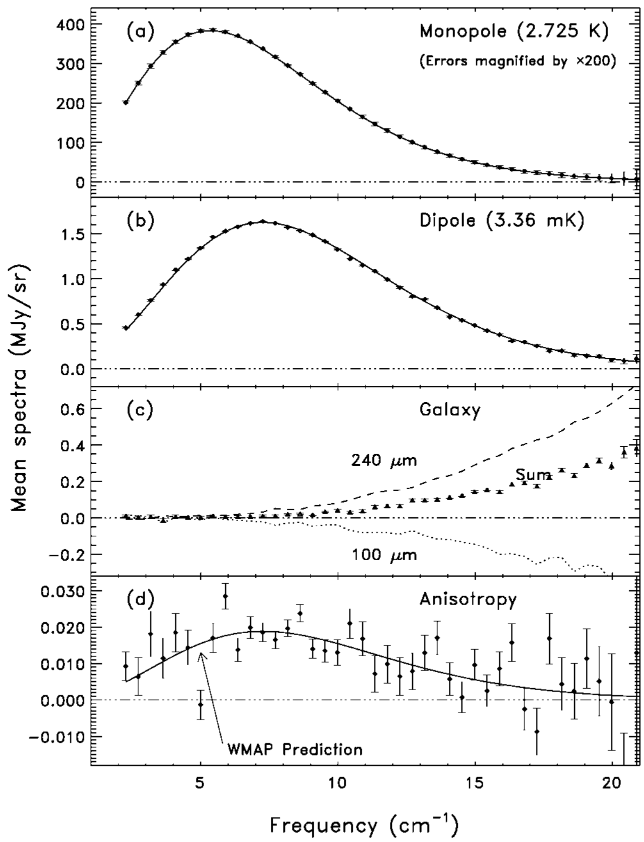

FIG. 1.—Spectra resulting from the fit to fixed spatial templates with 1 σ errors. (*a*) Monopole spectrum with errors magnified by a factor of 200; the curve is a 2.725 K Planck spectrum. (*b*) Dipole spectrum; the curve is a 3.36 mK differential Planck spectrum. (*c*) Galactic spectra; the dashed and dotted lines are the fits to the 240 and 100 μm maps, respectively, and the points are the sum. (*d*) Anisotropy spectrum; the curve is the 39 μK differential Planck spectrum predicted by *WMAP*.

pressed in the analysis because of the differences in the *WMAP* and FIRAS instruments and scan patterns.

A point near 5 cm^{-1} appears 4 σ below the prediction. In fact it is approximately 3 σ low (including the correlation of nearby points). It may also be seen in Figure 1 of Fixsen et al. (1997), but these are not independent; the same FIRAS data are used in the construction of both spectra. The probability that at least one point in the 43 point spectrum is at least this deviant is 10%, so it may be chance.

Figure 2 shows the anisotropy spectrum along with the *predicted* Planck spectrum based on the *WMAP* data alone. The data at different frequencies are mildly (~10%) correlated, which is accounted for in the spectral analysis.

If we *fit* the FIRAS spectrum to a Planck spectrum, $\alpha\partial B_\nu/\partial T$, we find correlated rms temperature fluctuations of $\alpha = 39.5 \pm 2.5$ μK compared with the *WMAP* value of 39 μK.

We can further analyze the spectrum a_ν to search for evidence of spectral distortions due to the Sunyaev-Zeldovich (SZ) effect (Zeldovich & Sunyaev 1969), or for signs of residual Galactic contamination. We fit a_ν to a model of the form $\alpha\partial B_\nu/\partial T + \beta(-1/2T_0)Y_\nu + \gamma g\nu^2 B_\nu(T_D)$, where $Y(\nu,\ T_0) = B(\nu,\ T_0)x/(1 - e^{-x})[x/\tanh(x/2) - 4]$, $(x = h\nu/kT_0)$ and T_D is the dust temperature. The fit is not very sensitive to this temperature since the peak is far above the frequencies under consideration. Since the *WMAP* temperature map was normalized to have unit rms, α corresponds to the rms level of Planckian temperature anisotropy, β corresponds to the rms level of Sunyaev-Zeldovich

TABLE 1
CORRELATIONS OF FIT

	Uniform	Dipole	Dust (G)	Dust (H)	Anisotropy
Uniform	1.000	−0.017	0.341	−0.704	−0.162
Dipole	−0.017	1.000	0.084	−0.055	0.097
Dust (G)	0.341	0.084	1.000	−0.861	−0.096
Dust (H)	−0.704	−0.055	−0.860	1.000	0.140
Anisotropy	−0.162	0.097	−0.096	0.140	1.000

temperature anisotropy in the Rayleigh-Jeans limit, and γ corresponds to the rms level of dust emission relative to the emission at the Galactic poles, since the normalization z is chosen so the spectrum matches that at the Galactic poles. For $T_D =$ 15 K, $(\alpha,\ \beta,\ \gamma) = (39 \pm 3$ μK, 2 ± 6 μK, $0.012 \pm 0.014)$. The value of α is consistent with the measured *WMAP* rms of 39 μK. There is no evidence for Sunyaev-Zeldovich anisotropy or residual Galactic signal.

The five *WMAP* single-frequency rms fluctuation data at 22.77, 33.02, 40.72, 60.75, and 93.53 GHz can be fitted to the same templates and the results combined with the 43 point FIRAS spectrum a_ν to form a single 48 point spectrum. While some of the contamination is due to Galactic synchrotron and free-free emission, these are correlated to the dust so the dust templates remove much of it (for $|b| > 10°$). These spectra are fitted for α, β, and γ giving $(\alpha,\ \beta,\ \gamma) = (38.7 \pm 2.5$ μK, 0 ± 5 μK, $0.012 \pm 0.014)$, with $T_D = 15$ K. Treating the SZ coefficient as an upper limit, and assuming the SZ signal is uncorrelated with the primary anisotropy, we conclude that not more than 10/39, or 25%, of the *WMAP* variance could be due to distortions from the Sunyaev-Zeldovich effect at a 95% confidence level. This corresponds to an upper limit of $\Delta T = (10/39)^{1/2} \times 39$ μK $= 18$ μK, or $\Delta y = 3 \times 10^{-6}$ for rms fluctuations on a ~5° angular scale, consistent with the limit on a uniform SZ distortion of $|y| < 15 \times 10^{-6}$ (Mather et al. 1994) and the limit of SZ distortion by Bennett et al. (2003c). The limits obtained here make no assumption about the spatial distribution of the gas and are based on direct measurements of the spectrum in the Wien region, where the SZ distortion is manifest.

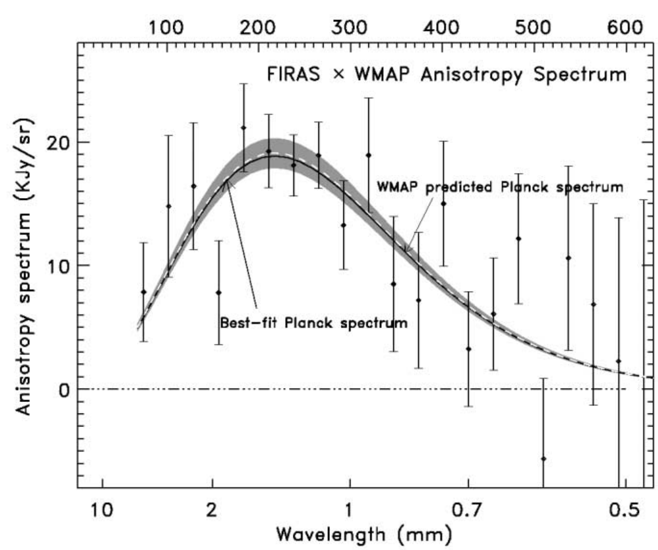

FIG. 2.—Mean anisotropy spectrum, as in Fig. 1*d*, with the points averaged in frequency. The uncertainties are 1 σ. The solid line is the differential Planck spectrum predicted by *WMAP*, and the dashed line with error band is the best-fit Planck spectrum.

The fit is also sensitive to dust above ∼5 K. A limit of 20% (95% confidence level) is placed on fraction of the *WMAP* temperature signal that can come from dust with a ν^2 dependence with a temperature above 5 K. This upper limit is about 1/2 of the CIB at 10 cm^{-1} (Fixsen et al. 1998).

4. CONCLUSIONS

The mean FIRAS spectrum of the anisotropy observed by *WMAP* is consistent with the Planck form, $\partial B/\partial T$, expected of CMB anisotropy. This result provides direct observational support for the widely held view that the signal detected by the *WMAP* is temperature anisotropy in the CMB.

We have used the anisotropy spectrum to place limits on the fraction of the *WMAP* signal that could be due to Comptonization by hot gas via the Sunyaev-Zeldovich effect or dust. We find that no more than 25% of the signal seen by *WMAP* could be due to the SZ effect or 20% due to dust at a 95% confidence level. This corresponds to an upper limit on rms fluctuations in the Compton y parameter of $\Delta y < 3 \times 10^{-6}$ on 5° angular scales and rules out models in which the anisotropy is primarily due to the SZ effect.

We thank N. Odegard for converting the *WMAP* data to Quadcube format and G. Hinshaw for helpful discussions. This work was supported by Science Systems and Applications, Inc.

REFERENCES

Bennett, C. L., et al. 1996, ApJ, 464, L1
———. 2003a, ApJ, 583, 1
———. 2003b, ApJS, 148, 1
———. 2003c, ApJS, 148, 97
COBE Diffuse Infrared Background Experiment (DIRBE) Explanatory Supplement. 1997, ed. M. G. Hauser, T. Kelsall, D. Leisawitz, & J. Weiland (*COBE* Ref. Publ. 97-A) (Greenbelt: NASA/GSFC), available in electronic form from the NSSDC
Fixsen, D. J., et al. 1994, ApJ, 420, 457
Fixsen, D. J., Cheng, E. S., Gale, J. M., Mather, J. C., Shafer, R. A., & Wright, E. L. 1996, ApJ, 473, 576
Fixsen, D. J., Dwek, E., Mather, J. C., Bennett, C. L., & Shafer, R. A. 1998, ApJ, 508, 123
Fixsen, D. J., Hinshaw, G., Bennett, C. L., & Mather, J. C. 1997, ApJ, 486, 623
Fixsen, D. J., & Mather, J. C. 2002, ApJ, 581, 817
Hinshaw, G., et al. 2003, ApJS, 148, 63
Mather, J. C., et al. 1994, ApJ, 420, 439
Mather, J. C., Fixsen, D. J., Shafer, R. A., Mosier, C., & Wilkinson, D. T. 1999, ApJ, 512, 511
O'Neill, E. M., & Laubscher, R. E. 1976, Extended Studies of a Quadrilateralized Spherical Cube Earth Data Base (Silver Spring: NEPRF Tech. Rep. 3-76; NTIS Rep. AD-A026294; Computer Sciences Corp. CSC/TR-76/6008)
Zeldovich, Ya. B., & Sunyaev, R. A. 1969, Ap&SS, 4, 301